

Magnetic profiles and coupling in Fe/Cr(110) superlattices

S.G.E. te Velthuis^{1,*}, G.P. Felcher¹, S. Kim², I.K. Schuller²

¹Materials Science Division/Intense Pulsed Neutron Source, Argonne National Laboratory, 9700 South Cass Ave, Argonne, IL 60439, USA

²Department of Physics, University of California – San Diego, La Jolla, CA 92093-0319, USA

Received: 7 August 2001/Accepted: 11 December 2001 – © Springer-Verlag 2002

Abstract. In epitaxial Fe/Cr superlattices the coupling between the Fe layers oscillates between antiferromagnetic (AFM) and ferromagnetic as a function of the Cr layer thickness t_{Cr} . The period of the oscillation is the same for superlattices grown with (211) and (100) orientations. We measured the coupling of Fe/Cr(110) superlattices consisting of three identical Fe layers. The magnetization curves were characterized by two to four levels, $M/M_s = \pm 1$ or $\pm \frac{1}{3}$. Polarized neutron reflectometry identified the direction of the magnetization of each Fe layer and showed that the levels $M/M_s = \pm \frac{1}{3}$ were not always due to AFM alignment of the central layer, but rather it was found that, in spite of the structural similarity, the bottom Fe layer had a different coupling strength from the top Fe layer. The magnetic coupling must be sensitive to small structural differences at the interface. Furthermore, the measurements indicate an unexpected periodicity for Fe/Cr(110) superlattices.

PACS: 61.12.He; 75.70.-i; 75.30.Et

The Fe/Cr system is one of the most thoroughly studied magnetic multilayer systems. A short and a long period of oscillatory coupling [1] are present between the Fe layers, depending on the Cr layer thickness. Recent experiments on Fe/Cr/Fe(001) trilayers [2, 3] show a 2 monolayer (ML) period modulated by long ($\sim 18 \text{ \AA}$) period oscillations. Multilayers are known to exhibit just long period oscillations, which are similar for epitaxial Fe/Cr(100), (211) [4], and (110)-textured polycrystalline [5] films, although highly strained Fe/Cr(110) [6] shows some differences. The origin of the long period in Fe/Cr is still not well understood, especially its apparent independence on growth orientation [7]. Therefore, we chose to investigate Fe/Cr(110), to now the least investigated due to technical difficulties in growing untwined, unfaceted, films [8].

Epitaxial Fe/Cr(110) films were grown by molecular beam epitaxy (MBE) on single crystal $\text{Al}_2\text{O}_3(110)$ substrates.

The Nb seed layers were grown at 500°C , followed by the Cr buffer layers at 300°C . Then three Fe layers, spaced by Cr layers, were deposited and protected by Cr/Nb double capping layers. In situ structural characterization using RHEED and LEED was performed at every stage of the growth. In these films, there is little evidence for twined or faceted growth in contrast to earlier publications [8]. All samples have a Fe layer thickness of 30 \AA . More details on the structural characteristics will be discussed in [9].

Samples with different Cr layer thicknesses (t_{Cr}) were investigated by SQUID magnetometry at 10K with the magnetic field H applied along the in plane [001] easy axis. Representative M - H loops are given in Fig. 1. The magnetization curves of the samples with $t_{\text{Cr}} = 12.3 \text{ \AA}$ and 17.6 \AA are similar in shape. In both cases, the total magnetization decreases from $M/M_s = +1$ to $\frac{1}{3}$ to $-\frac{1}{3}$ to -1 , for the descending field curve. Since the first step takes place at a positive field antiferromagnetic (AFM) coupling between the three Fe layers

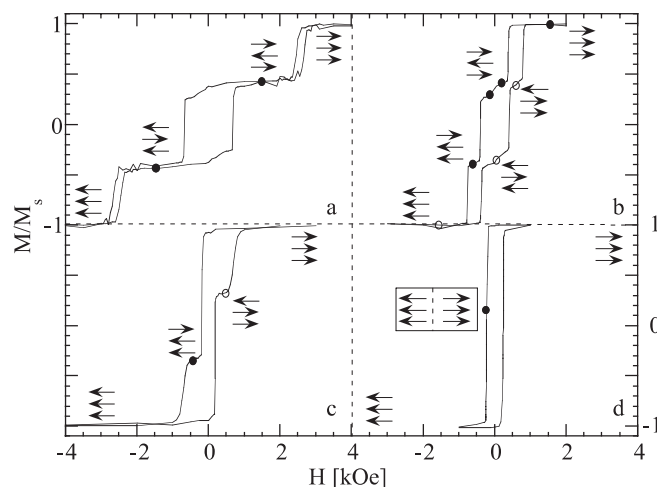


Fig. 1a–d. Magnetization curves, **a** $t_{\text{Cr}} = 12.3 \text{ \AA}$, **b** $t_{\text{Cr}} = 17.6 \text{ \AA}$, **c** $t_{\text{Cr}} = 23 \text{ \AA}$, **d** $t_{\text{Cr}} = 31 \text{ \AA}$. Arrows indicate the direction of the three Fe layer magnetizations as measured (●) or inferred (○) by symmetry at different fields by PNR. For (a), (c), and (d) the saturation configuration was measured at 5.4 kOe

*Corresponding author.

(Fax: +1-630/252-7777, E-mail: tevelthuis@anl.gov)

is implied. However, polarization neutron reflectivity (PNR) measurements [10], using the POSYI reflectometer at IPNS, showed that although the step sizes were the same for both samples, the reversal sequence was not.

In Fig. 1 the conditions in which PNR measurements were taken as well as the magnetic configurations fitting the data are indicated. A representation of how these configurations were obtained is given in Fig. 2. Here the measured and fitted spin asymmetry $(R^+ - R^-)/(R^+ + R^-)$ is shown as a function of incident neutron momentum k_0 perpendicular to the surface for $t_{Cr} = 17.6 \text{ \AA}$ at different applied fields. R^+ and R^- are the reflectivities for neutrons polarized parallel and antiparallel to the applied field, respectively. The orientations of Fe layer magnetizations as determined by the fits is given alongside the graph. The fits were obtained by manually varying the parameters that model the sample and calculating the reflectivity as described in [11]. The fits at different fields were made using the same parameters for the structural and non-magnetic scattering terms, and only the magnetizations were varied, although they were limited to lie along the applied field axis (polarization analysis measurements proved that the magnetization vectors were always collinear to the field). It is clear from this figure that PNR is very sensitive to the magnetization vectors of each individual Fe layer.

For $t_{Cr} = 12.3 \text{ \AA}$, after the step at $+1500 \text{ Oe}$ in a descending field, the central Fe layer has reversed in orientation, in order to minimize the exchange energy with the neighboring Fe layers. The relatively high field at which this transition takes place indicates that the AFM coupling is strong. After the step at -1500 Oe , all three layers have reversed their orientation in order to minimize the Zeeman energy while keeping the exchange energy minimal. At the last step, all three layers are again magnetized along the field direction.

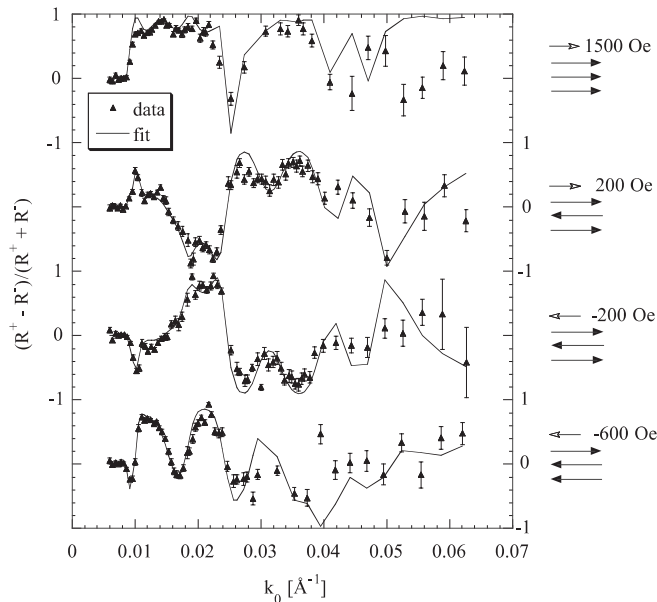


Fig. 2. The spin asymmetry as a function of incident neutron momentum for $t_{Cr} = 17.6 \text{ \AA}$ and the determined orientation of the Fe layer magnetizations. The difference in the spin asymmetry at $+200 \text{ Oe}$ and -200 Oe , is simply a difference in sign due to the switched sign of the applied field, which defines the “+” state of the neutron spin

For $t_{Cr} = 17.6 \text{ \AA}$ the first step in the magnetization is at a much lower field, indicating weaker, yet still AFM coupling. Unexpectedly, the PNR data revealed (Fig. 2) that after the step in the magnetization measured at -600 Oe , not all three Fe layers reversed their magnetization, but only the bottom one. In this case, the Zeeman energy was sufficient to break the AFM alignment between the bottom two layers. This led to the conclusion that the coupling strength between the middle and bottom Fe layer is weaker than that between the top and middle layer.

The $M-H$ loop for $t_{Cr} = 23 \text{ \AA}$ shows only two steps. After the first measured at $H = -550 \text{ Oe}$, the two bottom layers had reversed their magnetization, indicating ferromagnetic (FM) coupling between these two layers. Since the field necessary to switch the top layer is larger, it is surmised that an AFM coupling exists between top and middle layer.

PNR measurement with polarization analysis were also performed during the steps in the magnetization for all samples. In most cases the spin-flip reflectivities were zero, indicating that also during the reversal of the layers, the magnetization was along the applied field axis. The exception is for $t_{Cr} = 12.3 \text{ \AA}$, where some spin-flip scattering was measured at the onset of the step going from $\frac{1}{3}$ to $-\frac{1}{3}$ at fields of -0.6 and -0.65 kOe , indicating a component of the magnetization perpendicular to the applied field. As mentioned above, during this step all three Fe layers reverse their magnetization, while keeping an AFM alignment. Apparently this reversal is characterized by a rotation process instead of reverse domain nucleation followed by domain wall propagation.

In the case of $t_{Cr} = 31 \text{ \AA}$, the magnetization curve indicated that all three layers switched at the same field, which means that they are either uncoupled or ferromagnetically coupled. To distinguish between the two situations, a variety of PNR measurements was undertaken. Polarization an-

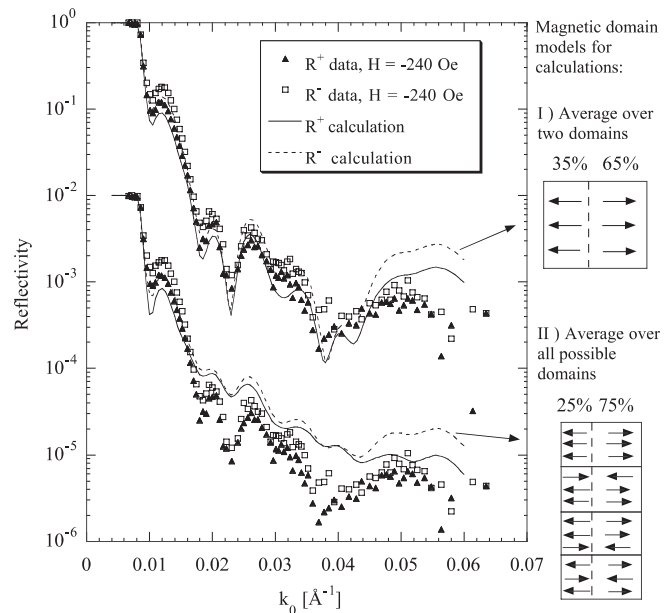


Fig. 3. The spin dependent reflectivities as a function of incident neutron momentum for $t_{Cr} = 31 \text{ \AA}$ measured with the field along the easy axis. The same data is compared to two calculations, each assuming a mixture of domains. The top model best corresponds to the data

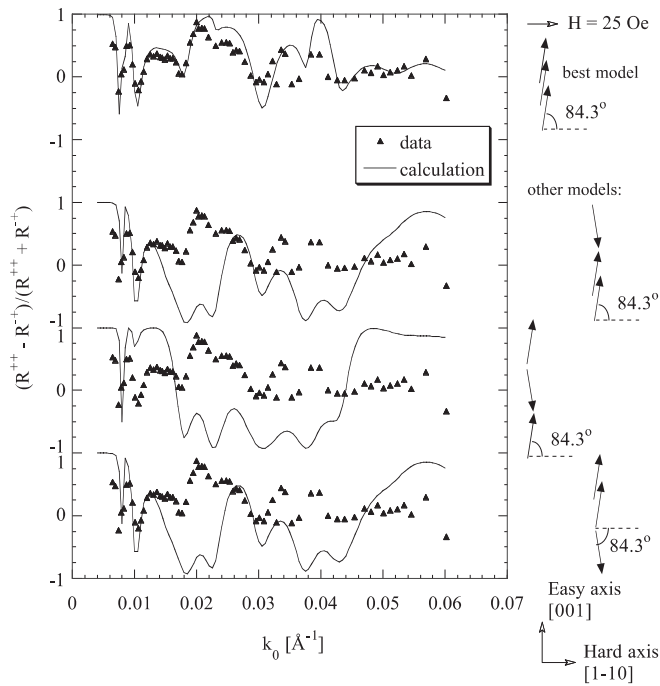


Fig. 4. The $(R^{++} - R^{-+})/(R^{++} + R^{-+})$ as a function of incident neutron momentum for $t_{\text{Cr}} = 31 \text{ \AA}$ measured with the field along the *hard axis*. The same data is compared to four calculations. The top one best represents the data

alysis measurements close to the reversal field (-240 Oe), where $M/M_s \sim 0$, indicated that all magnetization vectors are collinear to the applied field. Therefore, the reversal most likely takes place through domain nucleation and domain wall movement. If no coupling were present between the layers, reverse domains in each Fe layer would form at random during the reversal. On the other hand, if the layers are FM coupled, the magnetization vectors of all three layers will always be parallel. Figure 3 indicates that this is the configuration that best describes the experimental data.

In a second experiment, a magnetic field of 5.4 kOe was initially applied along the in plane hard magnetic axis $[1\bar{1}0]$, and then lowered to 25 Oe ; a field sufficient to keep the neutrons polarized, while the magnetization of the Fe layers become aligned along the perpendicular $[001]$ easy axis. If the layers were uncoupled, their respective magnetization is expected to be random, while if they are coupled, they should be parallel to each other. Figure 4 shows the results of polarization analysis. Here the quantity $(R^{++} - R^{-+})/(R^{++} + R^{-+})$

is compared to calculations for four models. It is clear that only a model in which the three layers are ferromagnetically aligned describes the data.

In conclusion, PNR measurements on epitaxial Fe/Cr (110) superlattices identified the orientation of the layer magnetizations at different stages of the hysteresis curves. It was found that although the layers are supposed to be identical based on structural studies and growth conditions, they are not the same magnetically. In the weaker coupled systems the bottom Fe layer had a different coupling strength with respect to the middle layer than the top Fe layer, a feature that could have caused ambiguities of determination of the coupling strength if only magnetic measurements were available. Therefore, the magnetic coupling must depend very delicately on small structural differences at the interfaces. The coupling in these four samples was found to be: strong AFM for $t_{\text{Cr}} = 12.3 \text{ \AA}$, weaker AFM for $t_{\text{Cr}} = 17.6 \text{ \AA}$ (but with two different strengths), FM and AFM for $t_{\text{Cr}} = 23 \text{ \AA}$, and weakly FM for $t_{\text{Cr}} = 17.6 \text{ \AA}$. As a comparison, in Fe/Cr(100) and (211) superlattices, for $t_{\text{Cr}} = 12.3 \text{ \AA}$ the coupling is AFM, $t_{\text{Cr}} = 17.6 \text{ \AA}$ and 23 \AA are at the two edges of the FM region, and $t_{\text{Cr}} = 31 \text{ \AA}$ corresponds to the center of the second AFM maximum. In other words, our results seem to indicate that the period of the oscillations is longer in Fe/Cr(110) compared to that found in Fe/Cr(100) and (211). A more detailed discussion of the coupling strengths will be presented elsewhere [9].

Acknowledgements. Work at Argonne was supported by the US DOE, Office of Science, Contract No. W-31-109-ENG-38. Work at UCSD was supported by the US DOE.

References

1. J. Unguris, R.J. Celotta, D.T. Pierce: Phys. Rev. Lett. **67**, 140 (1991)
2. C.M. Schmidt, D.E. Bürgler, D.M. Schaller, F. Meisinger, H.-J. Güntherodt: Phys. Rev. B **60**, 4158 (1999)
3. B. Heinrich, J.F. Cochran, T. Monchesky, R. Urban: Phys. Rev. B **59**, 14520 (1999)
4. E.E. Fullerton, M.J. Conover, J.E. Mattson, C.H. Sowers, S.D. Bader: Phys. Rev. B **48**, 15755 (1993)
5. S.S.P. Parkin, N. More, K.P. Roche: Phys. Rev. Lett. **64**, 2304 (1990)
6. H.J. Elmers, G. Liu, H. Fritzsche, U. Gradmann: Phys. Rev. B **52**, R696 (1995)
7. M.D. Stiles: J. Magn. Magn. Mater. **200**, 322 (1999)
8. W. Folkerts, F. Hakkens: J. Appl. Phys. **73**, 3922 (1993)
9. S. Kim, I.K. Schuller: unpublished
10. J.F. Ankner, G.P. Felcher: J. Magn. Magn. Mater. **200**, 741 (1999)
11. G.P. Felcher, R.O. Hilleke, R.K. Crawford, J. Haumann, R. Kleb, G. Ostrowski: Rev. Sci. Instrum. **58**, 609 (1987)